Rate Constants and Branching Ratios for the Reactions of Selected Atmospheric Primary Cations with *n*-Octane and Isooctane (2,2,4-Trimethylpentane)

Susan T. Arnold,[†] A. A. Viggiano, and Robert A. Morris*

Air Force Research Laboratory, Space Vehicles Directorate (AFRL/VSBP), 29 Randolph Road,
Hanscom AFB, Massachusetts 01731-3010

Received: June 30, 1997[⊗]

Gas-phase ion molecule reactions of the primary atmospheric cations (NO^+, O_2^+, O^+, N^+, and N_2^+) with two isomers of octane, n-C_8H_{18} and iso-C_8H_{18} (2,2,4-trimethylpentane) have been studied using a variable temperature selected ion flow tube instrument. Reaction rate constants and product branching fractions were measured from 300 to 500 K. The reactions of O_2^+, O^+, N^+, and N_2^+ with n-C_8H_{18} and iso-C_8H_{18} proceed at the collision rate via dissociative and/or nondissociative charge transfer. The NO^+ reactions occur primarily by hydride transfer; the reaction rate for the straight-chain isomer is only one-fourth the collision rate, while the reaction rate for the branched isomer is significantly enhanced. The reaction of *n*-octane with each atmospheric cation generates two to four major product ions and numerous minor species. The major ionic products are alkyl cations, $C_nH_{2n+1}^+$, where the degree of fragmentation of the hydrocarbon chain is governed largely by the reactant ion recombination energy. The largest ionic products observed, n-$C_8H_{17}^+$ and n-$C_8H_{18}^+$, thermally decompose at temperatures above 300 K. The reaction of isooctane with each atmospheric cation generates fewer minor species than was observed in the *n*-octane reactions, and only one to three major product ions are observed. The main ionic product of the O_2^+, O^+, N^+, and N_2^+ reactions is the alkyl cation $C_4H_9^+$, although several reactions also produce significant amounts of the related radical cation $C_4H_8^+$. The main ionic product of the NO^+ reaction, $C_8H_{17}^+$, thermally decomposes into $C_4H_9^+$ at temperatures above 300 K. Presumably, the specificity of the product ion formation in the iso-C_8H_{18} reactions is a consequence of the neutral reactant structure. Except for thermal fragmentation of $C_8H_m^+$ product ions at temperatures above 300 K, there is little temperature dependence on the product ion branching fractions for the reported reactions.

Introduction

The primary positive ions formed in the atmosphere, from a variety of ionization processes, are N_2^+, O_2^+, N^+, O^+, and NO^+. These ions are rapidly converted to O_2^+ and NO^+, which undergo further reactions with H_2O, eventually forming the stable proton hydrates, $H_3O^+(H_2O)_n$.[1] Much is known about the chemistry of the primary atmospheric cations with small organic molecules, including small hydrocarbons such as methane and ethane.[2] These ion−molecule reactions are of interest because of the important role they play in forming organic molecules found in interstellar clouds.[3]

To date, there has been little interest in the reactions of the primary atmospheric cations with larger aliphatic hydrocarbons. The extensive use, among radiation chemists, of NO and O_2 as charge and radical scavengers prompted several studies of the reactions of NO^+ and O_2^+ with C_3−C_8 alkanes.[4,5] Several NO^+ reactions were also reported among a larger survey of hydride transfer reactions involving linear, branched, and cyclic C_2−C_9 alkanes.[6] More recently, Smith et al.[7] examined reactions of NO^+ and O_2^+ with a number of hydrocarbons to determine the potential usefulness of these ions as chemical ionization agents for trace gas analysis of organic molecules found in air and human breath.

We have undertaken a more extensive study of the reactions of primary atmospheric cations with the larger alkanes commonly found in fuels such as gasoline or kerosene in order to explore the possibility that such ion−molecule reactions could be used to enhance the rate of combustion or ignition. The oxidation of hydrocarbons is a chain reaction process involving free radicals; the most difficult step is thought to be chain initiation, formation of the first radicals, because this involves either thermal decomposition of, or reaction between, relatively stable molecules. Once radical formation is initiated, the remaining steps in the process proceed with little to no activation energy. Over the years, it has been noted that small additions (sometimes even negligible traces) of certain compounds can have a dramatic effect on the rate of combustion.[8] Some additives act as accelerants by facilitating the formation of the first free radicals. Other additives have a retarding effect; they react rapidly with the initial radicals yielding in return only weakly reactive radicals that are incapable of propagating the chain reaction. Because ion−molecule reactions are typically 100 times faster than conventional combustion reactions, i.e., those between neutral species, they may affect the rate of combustion or ignition by breaking chemical bonds, creating radicals, and speeding up the first and slowest step in the combustion reaction. In this initial paper, we report the reaction rate constants and product branching fractions, from 300 to 500 K, for the reactions of NO^+, O_2^+, O^+, N^+, and N_2^+ with two isomers of octane: *n*-octane and isooctane (2,2,4-trimethyl pentane).

Experimental Section

The measurements were made using the Air Force Research Laboratory variable temperature-selected ion flow tube.[9] Instruments of this type have been the subject of review,[10] and only those aspects relevant to the present study will be discussed in detail.

[†] Under contract to Aerodyne Research, Inc., Billerica, MA.

* To whom correspondence should be addressed.

[⊗] Abstract published in *Advance ACS Abstracts,* November 15, 1997.

S1089-5639(97)02106-3 CCC: $14.00

All reactant ions were produced in a moderate pressure ion source (0.1−1 Torr) by electron impact on a precursor compound. The reactant ion species of interest was mass selected in a quadrupole mass filter and injected into the flow tube through a Venturi inlet. The reactant neutral was introduced downstream through a finger inlet, 1/8 in. stainless steel tubing which enters the flow tube perpendicular to the flow and terminates at the radial center of the flow tube with an elbow directing the added gas in the upstream direction. The reactant neutral gas reacted with the ions for a known reaction time (∼2 ms) in a fast flow of He buffer gas (∼100 m s^{-1}) which was maintained at a total pressure of ∼0.45 Torr. A small fraction of the gas in the tube flowed through a sampling orifice, and the reactant and product ions in this flow were mass analyzed in a second quadrupole mass filter and detected by a particle multiplier. Rate constants were extracted from least-squares fits of the logarithm of the reactant ion signal versus concentration of reactant neutral. The reaction time was determined from previous time-of-flight measurements. The accuracy of the measured overall rate constants is ±25%, and the relative accuracy is ±15%.[9]

Product branching fractions were determined by recording the product ion count rates as a function of the neutral reactant flow rate. To account for the effects of secondary reactions between the product ions and the reactant neutral, the reported branching fractions were determined by extrapolating the measured branching percentages to a neutral reactant flow rate of zero. Branching measurements were made by operating the mass spectrometer at both low- and high-resolution settings. The high-resolution data were used to determine the branching ratio between product ions of similar mass, and this ratio was applied to the low-resolution data (taken to minimize mass discrimination) wherein the species of similar mass appeared as a single broad peak. The absolute uncertainty in the branching data is difficult to estimate because the effects of mass discrimination and differential rates of diffusion were not quantified. However, these effects tend to cancel one another since both depend generally on mass but in opposite senses. Furthermore, differential diffusion is expected to be minimal for large ions in a He buffer, and the data taken under low resolution conditions were largely unaffected by mass discrimination as evidenced by the good agreement between reactant ion loss and product ion total: Comparing the reactant ion signal loss to the sum of the product ion signals yields a maximum absolute uncertainty in the branching fractions of 25%. For the major product ions, the branching fractions are reported to be precise to within 5 percentage points, while the precision is much better for the minor product ions. It should be noted that branching fractions of one or two percent could result from impurities and may not be significant.

The reactant gases, n-C_8H_{18} (99+ %) and iso-C_8H_{18} (99.8%), were obtained commercially and used without further purification; the maximum water content of these anhydrous samples was <0.005%. The He buffer gas (99.999%) was passed through a molecular sieve/liquid nitrogen trap to reduce residual water vapor. Precursor source gases that were used included NO for NO^+, O_2 for O^+ and O_2^+, and N_2 for N^+ and N_2^+. While we intend to investigate the reactivity of excited state ions, especially those of NO^+, such studies are beyond the scope of this initial report, and care was taken to minimize the formation of vibrationally and electronically excited reactant ions. The formation of NO^{+*} and O^{+*} (typically ∼2%) was monitored by introducing a small flow of N_2 into the flow tube, prior to introducing any octane reactants. Only the excited electronic states of NO^+ and O^+ charge transfer with N_2. The percentage of N^{+*} was not determined although source conditions were generally set to minimize production of excited electronic states. Vibrationally excited states of N_2^+ and NO^+ were quenched by introducing a small flow of N_2 into the tube upstream of the reaction zone.[11] The percentage of vibrationally excited O_2^+, typically ∼5%, was determined by monitoring the fast charge-transfer reaction of O_2^+ ($n > 0$) with Xe.

TABLE 1: Total Rate Constants, from 300 to 500 K, for the Reactions of Atmospheric Cations with *n*-Octane and Isooctane (2,2,4-Trimethylpentane). Rate Constants for Most Isooctane Reactions Were Measured Only at 300 and 500 K. Reaction Efficiencies Are Given in Parentheses

	total rate constant/(10^{-9} cm^3 s^{-1})		
reaction	300 K	400 K	500 K
$NO^+ + n\text{-}C_8H_{18} \rightarrow$ products	0.54 (28)	0.42 (22)	0.42 (22)
$NO^+ + \text{iso-}C_8H_{18} \rightarrow$ products	1.8 (95)	1.9 (100)	1.9 (100)
$O_2^+ + n\text{-}C_8H_{18} \rightarrow$ products	1.8 (95)	2.1 (110)	2.1 (110)
$O_2^+ + \text{iso-}C_8H_{18} \rightarrow$ products	1.8 (100)		2.3 (128)
$O^+ + n\text{-}C_8H_{18} \rightarrow$ products	2.3 (92)	2.5 (100)	2.9 (116)
$O^+ + \text{iso-}C_8H_{18} \rightarrow$ products	2.4 (96)		2.8 (112)
$N^+ + n\text{-}C_8H_{18} \rightarrow$ products	2.4 (92)	2.7 (104)	3.0 (115)
$N^+ + \text{iso-}C_8H_{18} \rightarrow$ products	2.4 (92)		3.1 (119)
$N_2^+ + n\text{-}C_8H_{18} \rightarrow$ products	2.0 (100)	2.0 (100)	2.1 (105)
$N_2^+ + \text{iso-}C_8H_{18} \rightarrow$ products	2.0 (100)		2.0 (100)

Results and Discussion

Rate constants and reaction efficiencies for the reactions of *n*-octane and 2,2,4-trimethylpentane (isooctane) with selected atmospheric cations are presented in Table 1. Collisional rate constants were calculated assuming a negligible dipole moment for each octane isomer and molecular polarizability values of 15.9 $Å^3$ for n-C_8H_{18} and 15.4 $Å^3$ for iso-C_8H_{18}.[12] Rate constants and product branching fractions for all n-C_8H_{18} reactions were measured at 300, 400, and 500 K. With the exception of the NO^+ reactions, all iso-C_8H_{18} reactions were studied only at 300 and 500 K since the rate constants and branching ratios demonstrated little temperature dependence.

Temperature-dependent product branching fractions for the reactions of both C_8H_{18} isomers with NO^+, O_2^+, O^+, N^+, and N_2^+ are presented in Tables 2−6, respectively. As noted previously, branching fractions of one or two percent could result from impurities, and may not be significant; however, 1−2% product fractions were included in the Tables because (a) in some cases these products became more abundant as the temperature was varied, and (b) in some cases there were numerous different products at the 1−2% level, the sum of which far exceeded the maximum level attributable to impurities. The detected ion products are shown, and the neutral products are inferred from published thermochemistry and conservation of the reaction constituents. The product ion structure is unknown for nearly all the reactions in Tables 2−6. The reactions of O_2^+, O^+, N^+, and N_2^+ all had a large number of ionic products in common; we therefore believe that these products are the result of dissociative and nondissociative charge transfer as distinguished from reactions which incorporate N or O into the ionic product. Also, in many cases two or more carbocation isomers may be formed, and isomerization may occur during or after the time the ions are produced. Nevertheless, we attempted to calculate reaction enthalpies for the most likely products. Reported thermochemistry is taken from Lias et al. unless otherwise noted.[13] All reaction channels were found to be very exothermic.

Reaction enthalpies in Tables 2−6 were calculated using the following assumptions: (1) *n*-octane reactions produce straight-chain ion and neutral products, and those ionic products accommodate the positive charge on secondary carbons; (2)

TABLE 2: Product Branching Fractions, from 300 to 500 K, for the Reaction of NO$^+$ with n-Octane and Isooctane. Detected Ion Products Are Listed with the Assumed Neutral Products. Reaction Enthalpies Were Calculated As Described in the Text

		product branching fraction		
	ΔH_{rxn} (kJ mol^{-1})	300 K	400 K	500 K
$NO^+ + n\text{-}C_8H_{18} \rightarrow C_8H_{17}^+ + HNO$	(−30)	62	63	3
$\rightarrow C_6H_{13}NH_3^+ + CH_2CO$	−340	9	3	1
$\rightarrow C_6H_{13}^+ + (NH_3 + CH_2CO)$	−166	0	0	3
$\rightarrow C_5H_{11}NH_3^+ + CH_3CHCO$	−377	18	5	2
$\rightarrow C_5H_{11}^+ + (NH_3 + CH_3CHCO)$	−115	3	15	56
$\rightarrow C_4H_9NH_3^+ + C_2H_5CHCO$	−387	8	4	0
$\rightarrow C_4H_9^+ + (NH_3 + C_2H_5CHCO)$	−108	0	10	30
$\rightarrow C_3H_7^+ + (CH_3NH_2 + C_2H_5CHCO)$	−105	0	0	5
$NO^+ + iso\text{-}C_8H_{18} \rightarrow C_8H_{17}^+ + HNO$	(−60)	91	32	0
$\rightarrow C_4H_9^+ + (C_4H_9NO)$		7	68	99
$\rightarrow C_3H_7^+ + (C_5H_{11}NO)$		2	0	1

TABLE 3: Product Branching Fractions, from 300 to 500 K, for the Reaction of O$_2$$^+$ with n-Octane and Isooctane. Detected Ion Products Are Listed with the Assumed Neutral Products. Reaction Enthalpies Were Calculated As Described in the Text

		product branching fraction		
	ΔH_{rxn} (kJ mol^{-1})	300 K	400 K	500 K
$O_2^+ + n\text{-}C_8H_{18} \rightarrow C_8H_{18}^+ + O_2$	−218	13	5	0
$\rightarrow C_8H_{17}^+ + (H + O_2)$	−92	2	1	0
$\rightarrow C_8H_{16}^+ + (H_2 + O_2)$	{−195}	1	0	0
$\rightarrow C_6H_{13}^+ + (C_2H_5 + O_2)$	{−135}	31	32	29
$\rightarrow C_6H_{12}^+ + (C_2H_6 + O_2)$	{−225}	7	9	7
$\rightarrow C_5H_{11}^+ + (C_3H_7 + O_2)$	{−128}	17	19	17
$\rightarrow C_5H_{10}^+ + (C_3H_8 + O_2)$	{−219}	9	5	8
$\rightarrow C_4H_9^+ + (C_4H_9 + O_2)$	{−118}	5	9	13
$\rightarrow C_4H_8^+ + (C_4H_{10} + O_2)$	{−215}	6	10	10
$\rightarrow C_3H_7^+ + (C_5H_{11} + O_2)$	{−105}	4	6	10
$\rightarrow C_3H_6^+ + (C_5H_{12} + O_2)$	−144	2	2	2
$\rightarrow C_3H_5^+ + (C_5H_{12} + HO_2)$	{−135}	1	2	3
$O_2^+ + iso\text{-}C_8H_{18} \rightarrow C_8H_{17}^+ + (H + O_2)$	−124	2		1
$\rightarrow C_8H_{16}^+ + (H_2 + O_2)$	(−178)	2		0
$\rightarrow C_7H_{15}^+ + (CH_3 + O_2)$	−161	7		1
$\rightarrow C_5H_{11}^+ + (C_3H_7 + O_2)$	−39	1		0
$\rightarrow C_4H_9^+ + (C_4H_9 + O_2)$	−164	44		57
$\rightarrow C_4H_8^+ + (C_4H_{10} + O_2)$	(−188)	40		39
$\rightarrow C_3H_7^+ + (C_5H_{11} + O_2)$	−95	2		1
$\rightarrow C_3H_5^+ + (C_5H_{12} + HO_2)$	−115	2		1

TABLE 4: Product Branching Fractions, from 300 to 500 K, for the Reaction of O$^+$ with n-Octane and Isooctane. Detected Ion Products Are Listed with the Assumed Neutral Products. Reaction Enthalpies Were Calculated As Described in the Text

		product branching fraction		
	ΔH_{rxn} (kJ mol^{-1})	300 K	400 K	500 K
$O^+ + n\text{-}C_8H_{18} \rightarrow C_8H_{18}^+ + O$	−366	2	0	0
$\rightarrow C_8H_{17}^+ + OH$	(−699)	3	1	0
$\rightarrow C_8H_{16}^+ + (H_2 + O)$	{−343}	2	0	0
$\rightarrow C_6H_{13}^+ + (C_2H_5 + O)$	−283	2	1	2
$\rightarrow C_6H_{12}^+ + (C_2H_6 + O)$	{−373}	1	1	2
$\rightarrow C_6H_{11}^+ + (C_2H_5 + H_2 + O)$	−272	0	0	2
$\rightarrow C_5H_{11}^+ + (C_3H_7 + O)$	{−277}	4	3	4
$\rightarrow C_5H_{10}^+ + (C_3H_8 + O)$	{−367}	3	1	3
$\rightarrow C_5H_9^+ + (C_3H_7 + H_2 + O)$	−199	0	2	2
$\rightarrow C_4H_9^+ + (C_4H_9 + O)$	{−267}	21	21	16
$\rightarrow C_4H_8^+ + (C_4H_{10} + O)$	{−363}	8	6	6
$\rightarrow C_4H_7^+ + (C_4H_9 + H_2 + O)$	−188	0	3	5
$\rightarrow C_3H_7^+ + (C_5H_{11} + O)$	{−253}	42	50	43
$\rightarrow C_3H_6^+ + (C_5H_{12} + O)$	−293	7	6	7
$\rightarrow C_3H_5^+ + (C_5H_{11} + H_2 + O)$	−95	5	5	8
$O^+ + iso\text{-}C_8H_{18} \rightarrow C_5H_{11}^+ + (C_3H_7 + O)$	−188	1		2
$\rightarrow C_4H_9^+ + (C_4H_9 + O)$	−312	78		75
$\rightarrow C_4H_8^+ + (C_4H_{10} + O)$	−336	8		7
$\rightarrow C_4H_7^+ + (C_4H_9 + H_2 + O)$	−123	1		1
$\rightarrow C_3H_7^+ + (C_5H_{11} + O)$	−244	10		11
$\rightarrow C_3H_5^+ + (C_5H_{11} + H_2 + O)$	−74	2		4

isooctane reactions produce branched ion and neutral products with complimentary structures, i.e., no rearrangement of the C−C bonds occurs. Reaction enthalpies shown in ( ) are estimated values. When the product ion heat of formation was not available, it was estimated by comparison with similar ions or structures. The heat of formation for n-$C_8H_{17}^+$ (assumed 2-$C_8H_{17}^+$) was estimated to be 647 kJ mol^{-1} from a linear extrapolation of the heats of formation of smaller straight-chain hydrocarbon ions ($n = 3-7$). The heat of formation for the iso-$C_8H_{17}^+$ isomer was estimated by noting that ΔH_f for iso-$C_7H_{15}^+$ [of the form $(CH_3)_3CC(CH_3)_2^+$] is approximately 10% less than ΔH_f for the straight-chain isomer 2-$C_7H_{15}^+$. This

TABLE 5: Product Branching Fractions, from 300 to 500 K, for the Reaction of N^+ with *n*-Octane and Isooctane. Detected Ion Products Are Listed with the Assumed Neutral Products. Reaction Enthalpies Were Calculated As Described in the Text

		product branching fraction		
	ΔH_{rxn} (kJ mol^{-1})	300 K	400 K	500 K
$N^+ + n\text{-}C_8H_{18} \rightarrow C_8H_{18}^+ + N$	−455	2	1	0
$\rightarrow C_8H_{17}^+ + NH$	−643	3	0	0
$\rightarrow C_8H_{16}^+ + (H_2 + N)$	−329	1	0	0
$\rightarrow C_6H_{13}^+ + (C_2H_5 + N)$	−372	14	15	10
$\rightarrow C_6H_{12}^+ + (C_2H_6 + N)$	{−462}	3	3	2
$\rightarrow C_5H_{11}^+ + (C_3H_7 + N)$	{−365}	13	13	10
$\rightarrow C_5H_{10}^+ + (C_3H_8 + N)$	{−456}	5	5	5
$\rightarrow C_5H_9^+ + (C_3H_7 + H_2 + N)$	{−287}	0	1	1
$\rightarrow C_4H_9^+ + (C_4H_9 + N)$	{−355}	14	14	17
$\rightarrow C_4H_8^+ + (C_4H_{10} + N)$	{−452}	7	6	7
$\rightarrow C_4H_7^+ + (C_4H_9 + H_2 + N)$	{−276}	3	2	2
$\rightarrow C_3H_7^+ + (C_5H_{11} + N)$	{−342}	25	32	36
$\rightarrow C_3H_6^+ + (C_5H_{12} + N)$	−381	4	3	4
$\rightarrow C_3H_5^+ + (C_5H_{11} + H_2 + N)$	{−184}	6	5	6
$N^+ + \text{iso-}C_8H_{18} \rightarrow C_7H_{15}^+ + (CH_3 + N)$	−398	6		1
$\rightarrow C_6H_{13}^+ + (C_2H_5 + N)$	(−418)	0		1
$\rightarrow C_5H_{11}^+ + (C_3H_7 + N)$	−276	1		1
$\rightarrow C_4H_9^+ + (C_4H_9 + N)$	−401	52		64
$\rightarrow C_4H_8^+ + (C_4H_{10} + N)$	−425	26		16
$\rightarrow C_4H_7^+ + (C_4H_9 + H_2 + N)$	(−211)	1		1
$\rightarrow C_3H_7^+ + (C_5H_{11} + N)$	−332	7		8
$\rightarrow C_3H_6^+ + (C_5H_{12} + N)$	−373	1		1
$\rightarrow C_3H_5^+ + (C_5H_{11} + H_2 + N)$	−162	6		5

TABLE 6: Product Branching Fractions, from 300 to 500 K, for the Reaction of N_2^+ with *n*-Octane and Isooctane. Detected Ion Products Are Listed with the Assumed Neutral Products. Reaction Enthalpies Were Calculated As Described in the Text

		product branching fraction		
	ΔH_{rxn} (kJ mol^{-1})	300 K	400 K	500 K
$N_2^+ + n\text{-}C_8H_{18} \rightarrow C_8H_{18}^+ + N_2$	−556	1	1	0
$\rightarrow C_8H_{17}^+ + (H + N_2)$	(−430)	4	3	0
$\rightarrow C_8H_{16}^+ + (H_2 + N_2)$	{−532}	1	1	0
$\rightarrow C_6H_{13}^+ + (C_2H_5 + N_2)$	−473	1	0	0
$\rightarrow C_5H_{11}^+ + (C_3H_7 + N_2)$	−466	3	5	3
$\rightarrow C_5H_{10}^+ + (C_3H_8 + N_2)$	{−557}	0	1	1
$\rightarrow C_4H_9^+ + (C_4H_9 + N_2)$	{−456}	9	7	7
$\rightarrow C_4H_8^+ + (C_4H_{10} + N_2)$	{−553}	3	2	3
$\rightarrow C_4H_7^+ + (C_4H_9 + H_2 + N_2)$	{−377}	6	7	8
$\rightarrow C_3H_7^+ + (C_5H_{11} + N_2)$	{−443}	48	52	50
$\rightarrow C_3H_6^+ + (C_5H_{12} + N_2)$	−482	7	2	4
$\rightarrow C_3H_5^+ + (C_5H_{11} + H_2 + N_2)$	{−284}	17	19	24
$N_2^+ + \text{iso-}C_8H_{18} \rightarrow C_5H_{11}^+ + (C_3H_7 + N_2)$	−177	1		1
$\rightarrow C_4H_9^+ + (C_4H_9 + N_2)$	−501	41		37
$\rightarrow C_4H_8^+ + (C_4H_{10} + N_2)$	−526	6		2
$\rightarrow C_4H_7^+ + (C_4H_9 + H_2 + N_2)$	(−312)	1		2
$\rightarrow C_3H_7^+ + (C_5H_{11} + N_2)$	−433	25		32
$\rightarrow C_3H_6^+ + (C_5H_{12} + N_2)$	−473	1		0
$\rightarrow C_3H_5^+ + (C_5H_{11} + H_2 + N_2)$	−263	25		26

yields an estimate for ΔH_f (iso-$C_8H_{17}^+$) of 585 kJ mol^{-1}. Reaction enthalpies are shown in { } when product ions or neutrals could be one of several similar isomers. For example, *n*-octane reactions that produce straight chain alkenes could form isomers that differ only in the position of the C=C bond. The heats of formation for such isomers are generally within 5−10 kJ mol^{-1} of one another.

NO^+ Reactions

The reaction of NO^+ with isooctane proceeds at the collision rate. At 300 K the reaction produces primarily the hydride transfer product ion (> 90%):

$$NO^+ + \text{iso-}C_8H_{18} \rightarrow \text{iso-}C_8H_{17}^+ + HNO \qquad \Delta H \approx -60 \text{ kJ mol}^{-1} \quad (1)$$

At higher temperatures, the percentage of hydride transfer product ion decreases while the percentage of $C_4H_9^+$ simultaneously increases, as shown in Figure 1. An Arrhenius plot of this product channel rate constant (branching fraction of $C_4H_9^+$ multiplied by overall reaction rate constant) from 350 to 400 K yields an activation energy of 36 ± 3 kJ mol^{-1} for the formation of $C_4H_9^+$. Conceivably, the decrease in $C_8H_{17}^+$ signal, together with a simultaneous increase in $C_4H_9^+$ products, could indicate

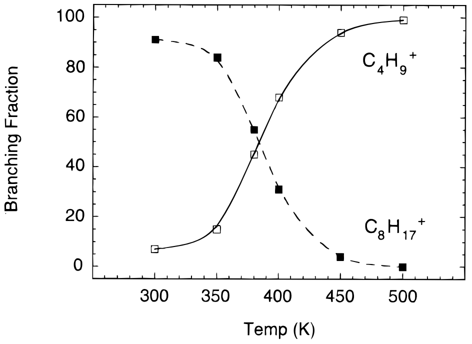

Figure 1. Temperature-dependent branching fractions for the reaction of NO^+ with isooctane.

a temperature-dependent competition between two different reaction channels, one that is exothermic and another that is endothermic yet becomes allowed at higher temperatures, either by increasing internal energy of the reactants or through the $T\Delta S$ term in the free energy expression. Note that the 36 kJ mol^{-1} activation energy for formation of $C_4H_9^+$ in reaction 1 is similar to the 32 kJ mol^{-1} endothermicity for that process. While this similarity is intriguing, and while we cannot rule out the above possibility, we believe that a more likely possibility is that the temperature-dependent branching fractions are the result of iso-$C_8H_{17}^+$ product ion thermal dissociation at higher temperatures:

$$\text{iso-}C_8H_{17}^+ \rightarrow C_4H_9^+ + C_4H_8 \qquad \Delta H \approx +92\ \text{kJ mol}^{-1} \quad (2)$$

The thermodynamics assumes the $C_4H_9^+$ thermal dissociation product is the *tert*-butyl carbocation. The evidence for this comes from the following experiment. We formed $C_8H_{17}^+$ in the ion source from iso-C_8H_{18} and selectively injected $C_8H_{17}^+$ into the flow tube. At 300 K essentially all the signal was $C_8H_{17}^+$. We then increased the temperature from 300 to 450 K and monitored the $C_8H_{17}^+$ and $C_4H_9^+$ signals. An 80% decrease in the $C_8H_{17}^+$ signal was observed, accompanied by a similar increase in the $C_4H_9^+$ signal, consistent with the thermal dissociation shown in reaction (2). Thus, we interpret the temperature-dependent branching fractions for the NO^+ reaction with isooctane to result from thermal dissociation of hydride transfer product ions. We do not believe the temperature-dependent branching ratios result from thermal decomposition of the neutral isooctane reactant because (1) the overall reaction rate does not depend on temperature, and (2) the iso-$C_8H_{17}^+$ ion was shown to thermally decompose at these temperatures, yielding a product distribution consistent with what is observed for the reaction of isooctane with NO^+.

The reaction of NO^+ with *n*-octane is the only reaction reported in this study that did not proceed at the collision rate; the reaction is only ~25% efficient over the temperature range of 300−500 K. This is consistent with earlier measurements of the reaction rate constant.[5,6] As previous researchers have noted, the probability that NO^+ will react with alkanes is greatly enhanced by branching within the molecule.[4,6]

We observe the reaction with *n*-octane to proceed primarily, although not exclusively, by hydride transfer at 300 K

$$NO^+ + n\text{-}C_8H_{18} \rightarrow n\text{-}C_8H_{17}^+ + HNO \qquad \Delta H \approx -30\ \text{kJ mol}^{-1} \quad (3)$$

The abrupt change in the *n*-$C_8H_{17}^+$ branching fraction between 400 and 500 K suggests the ion thermally dissociates at these temperatures, fragmenting into smaller $C_5H_{11}^+$ and $C_4H_9^+$ alkyl cations, analogous to the iso-$C_8H_{17}^+$ thermal dissociation discussed above. Thermal dissociation of $C_8H_{17}^+$ ions, formed from *n*-C_8H_{18}, has been observed previously at these temperatures by Matsuoka et al.,[5] and Lias et al. also reported observing dissociation of hydride transfer product ions for reactions of NO^+ with alkanes containing more than five carbon atoms.[6]

Previous studies have indicated that, aside from thermal dissociation, the only product channel in the reaction of NO^+ with *n*-alkanes is the hydride transfer channel.[6] However, we observe that nearly one-third of the reaction products at 300 K result from channels other than hydride transfer or thermal decomposition of hydride transfer product ions. In particular, product ions at 102, 88, and 74 amu are not thermal dissociation products of *n*-$C_8H_{17}^+$; their branching fractions decrease with increasing temperature between 300 and 400 K, before any decrease is observed in the *n*-$C_8H_{17}^+$ signal, and they do not correspond to $C_nH_{2n}^+$ or $C_nH_{2n+2}^+$ ions. Correlation between the loss of 88 and 74 amu ions and the increase in 71 and 57 amu ions suggests these products are of the form $C_nH_{2n+1}NH_3^+$, as shown in Table 2; e.g., 102 amu corresponds to $C_6H_{13}NH_3^+$, and the mass loss of 17 amu (from 88 to 71) is the loss of NH_3 from $C_5H_{11}NH_3^+$. The experiments do not address the structures of these protonated amines. The reaction channels yielding $C_nH_{2n+1}NH_3^+$ product ions and ketene and other related neutral products are quite exothermic. Presumably, the ions are stabilized at 300 K by collisions with the buffer gas; however, higher temperature increases the probability that the $C_nH_{2n+1}NH_3^+$ product ions themselves will dissociate into $C_nH_{2n+1}^+$ fragment ions and neutral NH_3 (or perhaps CH_3NH_2) molecules, which accounts for the observed increase in small alkyl fragment ions between 300 and 400 K. Unlike the other systems reported here, charge transfer between NO^+ and octane is endothermic, and therefore an intimate encounter is required in this case.

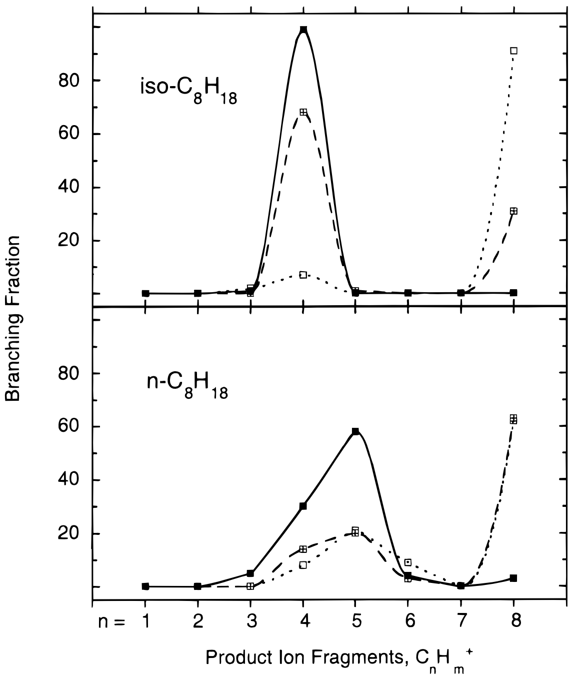

Figure 2. Branching fractions for all $C_nH_m^+$ fragment ions resulting from the reaction of *n*-octane or isooctane with NO^+ at 300 K (···), 400 K (- - -), and 500 K (—).

To examine the degree of hydrocarbon fragmentation by various primary atmospheric cations, it is somewhat useful to focus on the carbon chain-length of the product ions, rather than the individual product ions themselves. The branching fractions for all $C_nH_m^+$ fragment ions resulting from NO^+ reactions with both octane isomers at 300 and 500 K are shown in Figure 2 as a function of *n*. In the isooctane reaction, the extent of hydrocarbon fragmentation changes dramatically with temperature. Thermal decomposition of iso-$C_8H_{17}^+$ into $C_4H_9^+$ occurs over the entire temperature range from 300 to 500 K. In contrast, *n*-$C_8H_{17}^+$ product ions, from the reaction with *n*-octane, decompose only at temperatures above 400 K. In addition, several different fragment ions result from *n*-$C_8H_m^+$ decomposition, including primarily $C_5H_m^+$ fragments.

O_2^+ Reactions

The reaction of O_2^+ with isooctane proceeds at the collision rate via dissociative charge transfer, forming primarily $C_4H_9^+$

and $C_4H_8^+$ product ions.

$$O_2^+ + \text{iso-}C_8H_{18} \rightarrow C_4H_9^+ + (C_4H_9 + O_2) \qquad \Delta H \approx -164 \text{ kJ mol}^{-1} \quad (4a)$$

$$\rightarrow C_4H_8^+ + (C_4H_{10} + O_2) \qquad \Delta H \approx -188 \text{ kJ mol}^{-1} \quad (4b)$$

While the ratio of these two products is near unity at 300 K (each with a 40−44% branching fraction), a larger percentage of $C_4H_9^+$ is observed at higher temperatures, as the minor channel large mass product ions, $C_8H_m^+$, appear to thermally dissociate.

A secondary reaction channel was also observed between isooctane and the radical cation $C_4H_8^+$ which react to form $C_4H_9^+$ and neutral C_8H_{17}, or fragments thereof.

$$C_4H_8^+ + \text{iso-}C_8H_{18} \rightarrow C_4H_9^+ + C_8H_{17} \qquad \Delta H \approx ? \quad (5)$$

Since initial product structures are not known and isomerization may occur during or after the time the ions are produced, ΔH for reaction (5) was not estimated. However, formation of a C_8H_{17} radical, as proposed in reaction (5), is not unwarranted. The stability of alkyl radicals increases with carbon chain-length, and tertiary carbon radicals are more stable than secondary and primary radicals. A lower limit of −30 kJ mol^{-1} can be estimated for the C_8H_{17} radical heat of formation from a linear extrapolation of the heats of formation of smaller secondary carbon radicals ($n = 3-6$).[14]

The reaction of O_2^+ with n-octane proceeds at the collision rate via both dissociative and nondissociative charge transfer. The direct charge-transfer product ion, $C_8H_{18}^+$, is observed at 300 K (~13% branching fraction).

$$O_2^+ + n\text{-}C_8H_{18} \rightarrow C_8H_{18}^+ + O_2 \qquad \Delta H = -218 \text{ kJ mol}^{-1} \quad (6)$$

The $C_8H_{18}^+$ ion appears to thermally dissociate at temperatures above 400 K, similar to other $C_8H_m^+$ ions already discussed. In a previous study of this reaction Matsuoka et al.,[5] using time-resolved atmospheric pressure ionization spectrometry, also observed thermal decomposition of the $C_8H_{18}^+$ ion. They reported an activation energy of 15 kcal mol^{-1} (63 kJ mol^{-1}) and a thermal decomposition rate constant of (7.1×10^{11}) exp($-7500/T$) s^{-1} over the temperature range 398−483 K. In contrast to the present study, the authors report that $C_8H_{18}^+$ is the predominant product ion for this reaction at 300 K, with a branching fraction of over 90%. They reported the branching fraction for $C_8H_{18}^+$ decreased to 25% at 476 K. The difference in product branching ratios between these two measurements is likely due to a pressure effect; the charge-transfer product ion, $C_8H_{18}^+$, is probably stabilized more rapidly at atmospheric pressures than it is in the flow tube at ~0.5 Torr.

The O_2^+ reaction with n-octane yields more numerous, and more significant, dissociative charge-transfer product ions than were observed in the reaction of the branched octane isomer. Significant product ions are observed as $C_3H_m^+ - C_6H_m^+$ fragments and include both alkyl and radical product ions, although the formation of alkyl cations is favored over the formation of radical ions. None of the ions, $C_6H_m^+$ or smaller, appears to thermally dissociate at 500 K. The branching fractions for each ion fragment, $C_nH_m^+$, are shown in Figure 3 for the reactions of O_2^+, O^+, N^+, and N_2^+ with both isomers of octane. The figure illustrates how the O_2^+ reactant selectively breaks the isooctane molecule "in half", i.e., selectively forming $C_4H_m^+$ ions, while there is less selectivity in the n-octane reaction. The n-octane reaction slightly favors formation of $C_6H_m^+$ ion fragments over that of $C_5H_m^+$ and $C_4H_m^+$ ions, which are themselves favored over $C_3H_m^+$ ions. The product branching fraction changes with increasing temperature, as the large $C_8H_m^+$ ions thermally decompose, apparently fragmenting into $C_3H_m^+$ and $C_4H_m^+$ ions.

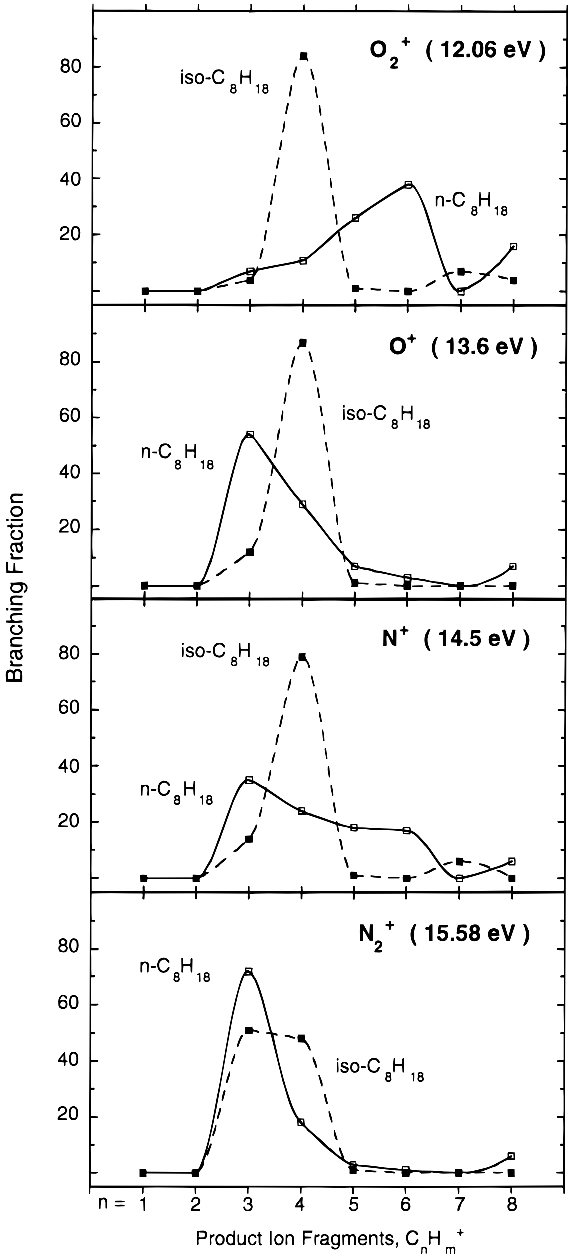

Figure 3. Branching fractions for all $C_nH_m^+$ fragment ions resulting from the reactions of n-octane (—) and isooctane (- - -) with O_2^+, O^+, N^+, and N_2^+ at 300 K. Reactant ion recombination energies are also shown.

O^+ Reactions

The reaction of O^+ with isooctane proceeds at the collision rate via dissociative charge transfer. There is essentially no change in the product branching fractions over the temperature range 300−500 K. As shown in Figure 3, the reaction heavily favors the formation of $C_4H_m^+$ ions (~85%), with a smaller amount (~15%) of $C_3H_m^+$ ions being formed as well. The dominant product channel (more than 75%) is that which produces the $C_4H_9^+$ ion.

$$O^+ + \text{iso-}C_8H_{18} \rightarrow C_4H_9^+ + (C_4H_9 + O) \quad \Delta H \approx -312 \text{ kJ mol}^{-1} \quad (7)$$

The reaction of O^+ with *n*-octane also proceeds at the collision rate predominantly via dissociative charge transfer. The dominant product ions are $C_4H_9^+$ and $C_3H_7^+$

$$O^+ + n\text{-}C_8H_{18} \rightarrow C_4H_9^+ + (C_4H_9 + O) \quad \Delta H \approx -267 \text{ kJ mol}^{-1} \quad (8a)$$

$$\rightarrow C_3H_7^+ + (C_5H_{11} + O) \quad \Delta H \approx -253 \text{ kJ mol}^{-1} \quad (8b)$$

Unlike the reaction with the branched isomer, the *n*-C_8H_{18} reaction also yields a host of minor product ions. Both alkyl and unsaturated hydrocarbon product ions are observed, although the formation of alkyl cations is favored. Except for the assumed thermal dissociation of the largest ions at higher temperatures, there is little temperature dependence of the product branching fractions. As shown in Figure 3, the more energetic O^+ reactant ion breaks the straight chain octane isomer into smaller product ions than were observed in the O_2^+ reactions. The O^+ reaction produces on average ~58% $C_3H_m^+$ ions, ~29% $C_4H_m^+$ ions, and significantly smaller amounts of the larger ions.

N^+ Reactions

The reaction of N^+ with isooctane proceeds at the collision rate via dissociative charge transfer, forming predominantly the $C_4H_m^+$ ions, $C_4H_9^+$ and $C_4H_8^+$.

$$N^+ + \text{iso-}C_8H_{18} \rightarrow C_4H_9^+ + (C_4H_9 + N) \quad \Delta H \approx -401 \text{ kJ mol}^{-1} \quad (9a)$$

$$\rightarrow C_4H_8^+ + (C_4H_{10} + N) \quad \Delta H \approx -425 \text{ kJ mol}^{-1} \quad (9b)$$

At 300 K, formation of the alkyl cation is favored 2:1 over formation of the radical cation, and this difference is magnified at higher temperatures, where the ratio becomes 4:1. The N^+ reaction also produces a smaller amount (~15%) of $C_3H_m^+$ ions.

The reaction of N^+ with *n*-octane also proceeds at the collision rate primarily via dissociative charge transfer, yielding as many as 14 different product ions. The major product ions are all alkyl cations.

$$N^+ + n\text{-}C_8H_{18} \rightarrow C_6H_{13}^+ + (C_2H_5 + N) \quad \Delta H \approx -372 \text{ kJ mol}^{-1} \quad (10a)$$

$$\rightarrow C_5H_{11}^+ + (C_3H_7 + N) \quad \Delta H \approx -365 \text{ kJ mol}^{-1} \quad (10b)$$

$$\rightarrow C_4H_9^+ + (C_4H_9 + N) \quad \Delta H \approx -355 \text{ kJ mol}^{-1} \quad (10c)$$

$$\rightarrow C_3H_7^+ + (C_5H_{11} + N) \quad \Delta H \approx -342 \text{ kJ mol}^{-1} \quad (10d)$$

In general, the formation of $C_3H_m^+$ ions is slightly favored, as shown in Figure 3. A slight change in the product distribution is observed with increasing temperature as the largest ions, $C_8H_m^+$, thermally dissociate.

N_2^+ Reactions

The reaction of N_2^+ with isooctane proceeds at the collision rate via dissociative charge transfer, forming nearly equal amounts of $C_4H_m^+$ and $C_3H_m^+$ product ions, in contrast to the O_2^+, O^+, and N^+ reactants which heavily favored the $C_4H_m^+$ product ions. The most significant reaction channels are the following:

$$N_2^+ + \text{iso-}C_8H_{18} \rightarrow C_4H_9^+ + (C_4H_9 + N_2) \quad \Delta H \approx -501 \text{ kJ mol}^{-1} \quad (11a)$$

$$\rightarrow C_3H_7^+ + (C_5H_{11} + N_2) \quad \Delta H \approx -433 \text{ kJ mol}^{-1} \quad (11b)$$

$$\rightarrow C_3H_5^+ + (C_5H_{11} + H_2 + N_2) \quad \Delta H \approx -263 \text{ kJ mol}^{-1} \quad (11c)$$

N_2^+ has the largest recombination energy of the ions examined in this survey of octane reactions, and it is the only ion that produces significant amounts of the relatively small $C_3H_5^+$ ion.

The reaction of N_2^+ with *n*-octane also proceeds at the collision rate primarily via dissociative charge transfer. Although as many as 12 different product ions are observed in this reaction, the formation of $C_3H_m^+$ ions is heavily favored (~75% branching fraction), as shown in Figure 3. A smaller amount (~17%) of $C_4H_m^+$ product ions is also observed. The major product ions are $C_3H_7^+$ and $C_3H_5^+$.

$$N_2^+ + n\text{-}C_8H_{18} \rightarrow C_3H_7^+ + (C_5H_{11} + N_2) \quad \Delta H \approx -443 \text{ kJ mol}^{-1} \quad (12a)$$

$$\rightarrow C_3H_5^+ + (C_5H_{11} + H_2 + N_2) \quad \Delta H \approx -284 \text{ kJ mol}^{-1} \quad (12b)$$

There is essentially no change in the product branching ratios from 300 to 500 K for the reaction of N_2^+ with either *n*-octane or isooctane.

Summary and Conclusions

The reactions of O_2^+, O^+, N^+, and N_2^+ with both *n*-octane and isooctane all proceed at the collision rate via dissociative and/or nondissociative charge transfer. Except for the case of O_2^+ + *n*-octane, the nondissociative charge-transfer channels are very minor pathways. The ionization potential (IP) of O_2, O, N, and N_2 are all greater than the IP of the alkane isomers, so charge transfer is expected to be fast. All the reactions are highly exothermic, and although the neutral products are not characterized in this experiment, it is energetically possible for all major and minor reaction channels to yield a radical species, either a radical neutral or a radical ion. Because the IP of NO is less than the IP of both alkane isomers, the charge-transfer channel is not allowed. The NO^+ reactions occur primarily by hydride transfer. Although the reaction is only about 25% efficient for the straight-chain isomer, branching within the octane reactant neutral significantly enhances the reaction rate.

The nondissociative charge transfer and hydride transfer product ions appear to thermally dissociate; iso-$C_8H_{17}^+$ and *n*-$C_8H_{18}^+$ dissociate at temperatures above 300 K, and *n*-$C_8H_{17}^+$ dissociates above 400 K. Except for the thermal fragmentation of $C_8H_m^+$ and $C_nH_{2n+1}NH_3^+$ ions at higher temperatures, there is little temperature dependence of the product ion branching fractions for the reported reactions.

All reactions with isooctane produce between one and three major ions, and product ion formation is governed largely by the structure of the reactant neutral. NO^+ primarily forms iso-$C_8H_{17}^+$ which decomposes at higher temperatures to $C_4H_9^+$. The O_2^+, O^+, and N^+ reactants also break the isooctane isomer in half; the O^+ primarily forms the $C_4H_9^+$ alkyl cation, while O_2^+ and N^+ produce significant amounts of both the $C_4H_9^+$ alkyl ion and the closely related radical cation, $C_4H_8^+$. The competition between $C_4H_8^+$ and $C_4H_9^+$ product ion formation is presumably governed by the details of the potential energy surface and is beyond the scope of this paper. While N_2^+ also produces the $C_4H_9^+$ alkyl cation, it differs from the other ions in that the reaction also forms significant amounts of $C_3H_m^+$ fragment ions, especially the $C_3H_7^+$ alkyl cation and the $C_3H_5^+$ allyl cation.

All reactions with *n*-octane produce between two and four major product ions with numerous minor products; the extent of *n*-octane fragmentation appears to be a function of the reactant ion energy, as shown in Figure 3. In general, the major product ions are alkyl cations, $C_nH_{2n+1}^+$, $n = 3-6, 8$. Although $C_7H_m^+$ reaction products would be energetically allowed, none were observed. For O_2^+ (IP of $O_2 = 12.06$ eV), the reaction favors the formation of somewhat larger product ions (with corresponding small neutral products). For O^+ (IP of $O = 13.6$ eV), the reaction clearly favors the formation of smaller product ions. This trend is even more noticeable for N_2^+ (IP of $N_2 = 15.58$ eV). Interestingly, the N^+ reactions (IP of $N = 14.5$ eV) are not as selective for smaller product ions as would have been inferred from this trend.

Because there have been numerous studies on the reactivity of alkyl cations such as $C_3H_7^+$, $C_4H_9^+$, and $C_5H_{11}^+$ with branched and unbranched alkanes,[2] it is possible to suggest the terminal ions for the reactions reported here. For C_4-C_9 alkanes, the reactions with alkyl cations all occur via hydride transfer, implying that $C_8H_{17}^+$ will be the most significant terminal ion for all the octane reactions discussed in this report. However, since the $C_8H_{17}^+$ ions thermally dissociate at higher temperatures, the apparent terminal ions will be $C_4H_9^+$ for the iso-C_8H_{18} reactions and primarily $C_5H_{11}^+$, with some $C_4H_9^+$, for the *n*-C_8H_{18} reactions.

The products of the ion−molecule reactions reported here are precisely the type of radicals that would result from a conventional combustion initiation step involving thermal decomposition of alkanes at higher temperatures.[14,15] An important distinction is that the ion−molecule reaction rates are significantly faster and initiate radical formation at much lower temperatures. We plan to examine, through modeling, the possible role of "ion additives" in accelerating or initiating combustion. This initial survey of octane isomers is being extended to even larger alkane reactants, and additional studies are also underway to examine the reactivity of alkanes with other atmospheric cations, including the proton hydrates $H_3O^+(H_2O)_n$ and various excited-state ionic species. We also intend to study some of these ion−molecule reactions at much higher temperatures (temperatures limited by the thermal decomposition of the alkane of interest) using the Air Force Research Laboratory high-temperature flowing afterglow apparatus, which is capable of temperatures of up to 1800 K.[16]

Acknowledgment. We thank John Williamson and Paul Mundis for technical support. Helpful discussions with Michael Berman, Bish Ganguly, and Tim Edwards are gratefully acknowledged. The research was supported by the Air Force Office of Scientific Research.

References and Notes

(1) Viggiano, A. A.; Arnold, F. In *Atmospheric Electrodynamics*; Volland, H., Ed.; CRC Press: Boca Raton, 1995.

(2) Ikezoe, Y.; Matsuoka, S.; Takebe, M.; Viggiano, A. A. *Gas-Phase Ion−Molecule Reaction Rate Constants Through 1986*; Maruzen Company, Ltd.: Tokyo, 1987.

(3) Smith, D.; Adams, N. G. *Int. Rev. Phys. Chem.* **1981**, *1*, 271.

(4) Searles, S. K.; Sieck, W. *J. Chem. Phys.* **1970**, *53*, 794.

(5) Matsuoka, S.; Ikezoe, Y. *J. Phys. Chem.* **1988**, *92*, 1126.

(6) Lias, S. G.; Eyler, J. R.; Ausloos, P. *Int. J. Mass Spectrom. Ion Phys.* **1976**, *19*, 219.

(7) Smith, D.; Spanel, P. *Int. Rev. Phys. Chem.* **1996**, *15*, 231.

(8) Shtern, V. Y. *The Gas-Phase Oxidation of Hydrocarbons*; MacMillan: New York, 1964.

(9) Viggiano, A. A.; Morris, R. A.; Dale, F.; Paulson, J. F.; Giles, K.; Smith, D.; Su, T. *J. Chem. Phys.* **1990**, *93*, 1149.

(10) Smith, D.; Adams, N. G. *Adv. At. Mol. Phys.* **1988**, *24*, 1.

(11) Ferguson, E. E. *J. Phys. Chem.* **1986**, *90*, 731.

(12) Miller, T. M. In *CRC Handbook of Chemistry and Physics*; Lide, D. R., Ed.; CRC Press: Boca Raton, 1995.

(13) Lias, S. G.; Bartmess, J. E.; Liebman, J. F.; Holmes, J. L.; Levin, R. D.; Mallard, W. G. *J. Phys. Chem. Ref. Data* **1988**, *17, Supplement 1*, 1.

(14) Allara, D. L.; Shaw, R. *J. Phys. Chem. Ref. Data* **1980**, *9*, 523.

(15) Lindstedt, R. P.; Maurice, L. Q. *Combust. Sci. and Technol.* **1995**, *107*, 317.

(16) Hierl, P. M.; Friedman, J. F.; Miller, T. M.; Dotan, I.; Mendendez-Barreto, M.; Seeley, J.; Williamson, J. S.; Dale, F.; Mundis, P. L.; Morris, R. A.; Paulson, J. F.; Viggiano, A. A. *Rev. Sci. Inst.* **1996**, *67*, 149.